

# Sharpness Matching between Digital Image Display Devices

Hideaki HANEISHI,<sup>1</sup> Ritsuko OHTAKE,<sup>1</sup> Norimichi TSUMURA,<sup>1</sup> Yoichi MIYAKE,<sup>1</sup> Po-Chie HUNG,<sup>2</sup> Hans ROEHRIG<sup>3</sup> and William J. DALLAS<sup>3</sup>

<sup>1</sup>*Department of Information and Image Sciences, Chiba University, 1-33, Yayoi-cho, Inage-ku, Chiba, 263-8522 Japan,*

<sup>2</sup>*R&D Center, Konica Corporation, No. 1 Sakura-machi, Hino, Tokyo, 191 Japan,*

<sup>3</sup>*Department of Radiology, The University of Arizona, Tucson, AZ 85704, USA*

(Received January 22, 1998; Accepted April 9, 1998)

A method is presented for matching apparent sharpness between digital image display devices with different characteristics. The sharpness is most precisely described by the point spread function (PSF) as opposed to dot density such as DPI (dot per inch). The difference between devices is expressed as difference between transfer functions obtained from the PSFs. In the presented method, spatial frequency filtering for one digital image is carried out where the ratio of the transfer functions or its modified version is used as filter. The modification is introduced as a clipping operation to reduce excessive enhancement when the ratio of the transfer functions has a high pass characteristic with large gain. Through computer simulation including a subjective evaluation experiment and numerical evaluation, the effectiveness of filtering operation for sharpness matching is demonstrated.

**Key words:** sharpness matching, modulation transfer function, point spread function, computer simulation, CRT, film recorder

## 1. Introduction

Recently, various kinds of digital image display devices have become commercially available. Digital images captured by input devices such as cameras or scanners are stored in computers and then displayed on output devices such as CRTs, printers, film recorders, etc. In general, when an original digital image is displayed on different output devices, the image quality displayed is not necessarily identical. Lately, this mismatch in image quality has become a serious issue. Especially, in the color industry, the reproduction of device-independent color is strongly desired, and in fact, many techniques have been developed for this issue.<sup>1)</sup> The major factors in image quality, however, include not only color reproduction but also sharpness, noise graininess and so on. While color management between different devices has been discussed, it seems that fewer people pay attention to the mismatch in apparent sharpness and the work on this issue is quite sparse.<sup>2,3)</sup>

As a practical case, let us consider image diagnosis in medicine. Many images are provided in digital form such as CT, MRI and Computed Radiography. These images are recorded on a film and viewed by hanging them on light boxes. On the other hand, these images might be displayed on a high resolution CRT of a viewing terminal. At that time it would be desired that the image quality on the CRT, especially appearance of sharpness, is identical to that of the film.

Display devices we will treat here are those that can produce continuous tone at each pixel. The halftoning systems are excluded from our objective. The spatial resolution of digital image display devices is usually described by the number of dots per unit length such as DPI

(dot per inch). In this paper, when we compare the appearance of sharpness in two different devices, we assume a viewing condition such that the ratio of the distance between neighboring dots to the viewing distance, or in other words, the number of dots per unit viewing angle is constant. By introducing this condition, the difference in spatial resolution of individual devices is removed. Readers might think, under this condition, the appearance of sharpness is identical. However, this is not true because it depends not only on the number of dots per unit viewing angle but also on the width and shape of the spread of each dot, i.e., the point spread function (PSF).

On the basis of the above background, we propose a sharpness matching method. The proposed method is based on preprocessing for original images in digital form. Preprocessing is carried out using the concept of the inverse filter or its modified version as shown later. In Sect. 2, we first introduce the results of a preliminary experiment demonstrating how different point spread functions make observers perceive the difference in sharpness. In Sect. 3, we formulate the problem and proposed method mathematically. In Sect. 4, we show the computer simulation and evaluation results. In Sect. 5, we give some discussion on the applicability of the proposed method to real systems and the mathematical expression of a generalization.

## 2. Preliminary Experiment

We began our investigation by examining the PSFs of a few typical display devices. The examined devices include a film recorder used in the medical imaging and two high definition CRT monitors, A and B. The PSF of the film recorder was estimated from the reference.<sup>4)</sup> On the other hand, the PSFs of two CRTs were measured by displaying only one pixel and capturing its magnified image. The

E-mail: haneishi@ics.tj.chiba-u.ac.jp

display buffers of the CRT's A and B have addressable pixel matrixes of  $1280 \times 1024$  and  $2560 \times 2048$  pixels, respectively. We use the full width at half maximum intensity (FWHM) as a representation of the width of PSF. The width of measured PSF is normalized by the distance between neighboring pixels in order to represent units of pixels instead of physical scale. Table 1 shows the comparison of the width of the PSFs. The values for the CRTs were calculated from the cross section of PSFs when one pixel was displayed at center of the screen and with maximum luminance. The profiles of the cross sections used for the calculation are shown in Fig. 1. In fact, the

Table 1. Width of PSF of typical display devices.

Device	FWHM [pixel]
A film recorder	0.9
CRT A	1.8
CRT B	1.6

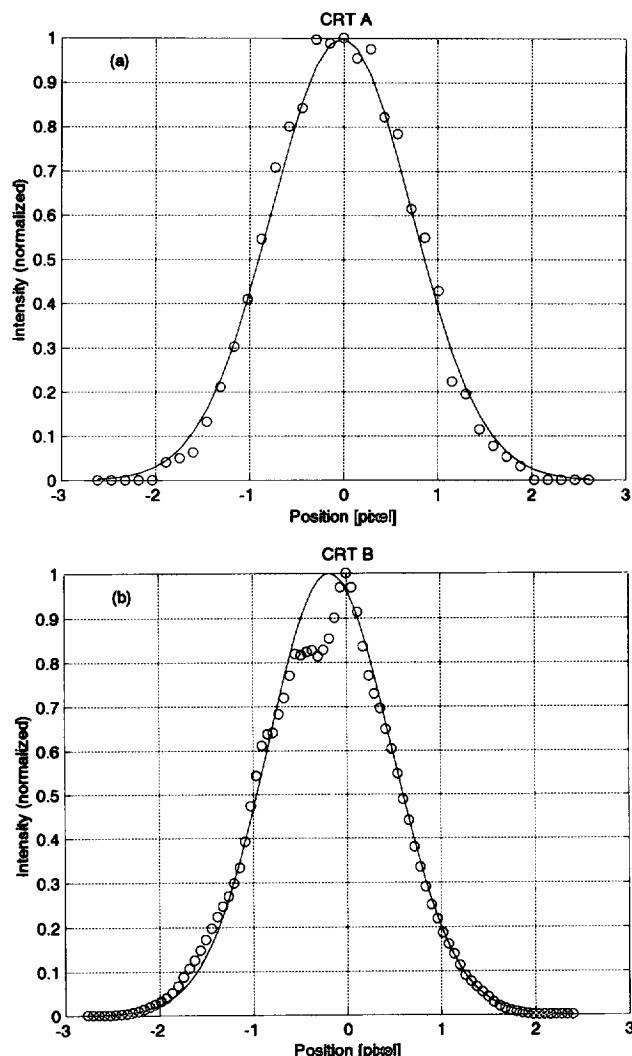


Fig. 1. Cross section of point spread function. (a) CRT A, (b) CRT B. The circles mean measured data and the solid lines mean Gaussian functions approximating the measured data.

PSFs of CRT B were measured for different positions and different luminance. The resultant statistics will be discussed in a later section. According to Table 1, while both CRTs are similar, the difference between the film recorder and CRTs is significantly large.

The larger the difference between the PSFs of two display devices is, the easier it becomes for observers to notice the difference. How large must the difference between PSFs be in order to make observers notice the difference in sharpness? To obtain the answer to this question, we carried out a simple, observer rating experiment using simulated images. We first prepared four original images shown in Fig. 2; 'flower,' 'characters,' 'building,' 'dog.' The size of each image is  $128 \times 128$  pixels. A displayed digital image is ideally modeled by the convolution between the discrete pixel array of original digital image and the continuous PSF. In the computer simulation, we first placed  $128 \times 128$  pixels of the original image on a  $512 \times 512$  square array sparsely as shown in Fig. 3(a). Next, we convolved them with a discrete PSF defined within a square block of  $21 \times 21$  pixels. A one-dimensional explanation of this procedure is shown in Fig. 3(b).

In this simulation we assumed that the PSF was given by a two-dimensional, symmetric Gaussian function. We defined two standard PSFs with FWHM of 1.32 and 1.86 [pixels]. For many display devices, approximation of the PSF by a Gaussian function is reasonable.<sup>5)</sup> In fact, Fig. 1 shows that the Gaussian function fits the measured PSFs of the CRTs well.

The CRT A mentioned above was used to display the simulated images. Prior to displaying the images, the non-linearity in the display function of the CRT was calibrated so that the output luminance was linear relative to the

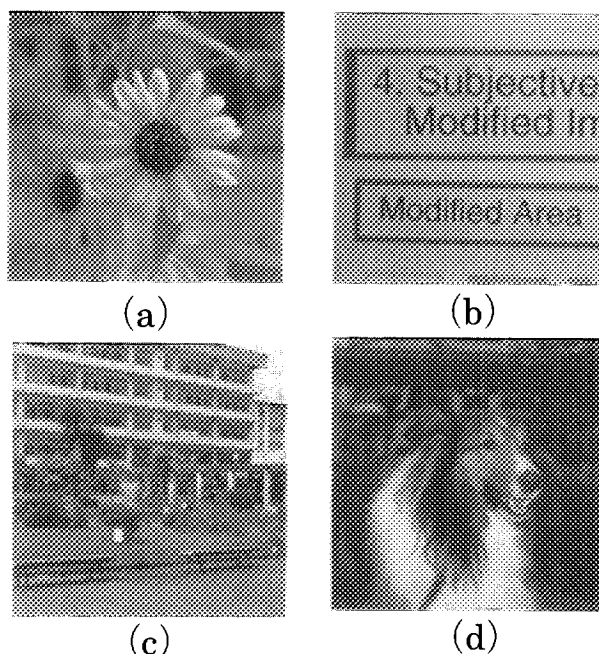


Fig. 2. Original images used in computer simulation and evaluation. (a) flower, (b) characters, (c) building, (d) dog.

input digital value.<sup>6)</sup> For each rating experiment, we displayed two simulated images simultaneously; one was an image convolved with the standard PSF, the other an image convolved with a slightly narrower or wider PSF. The width of the PSF for the latter image (called the test PSF) was gradually changed until

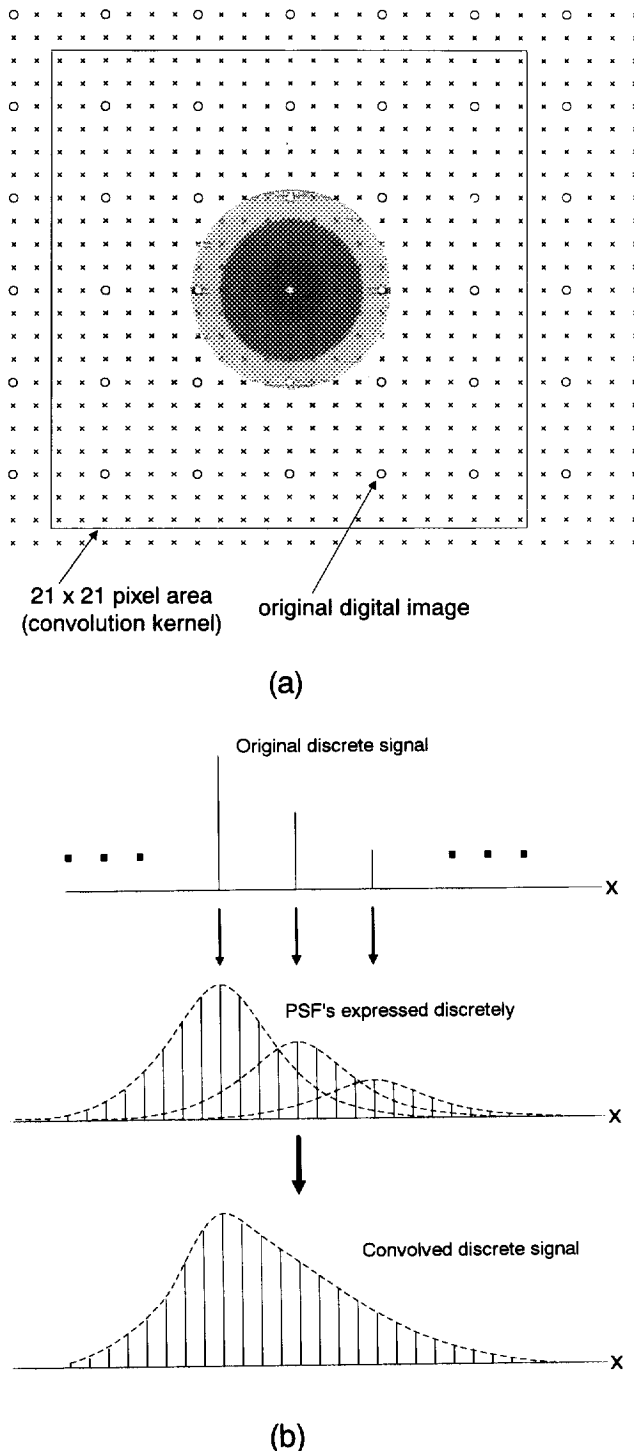


Fig. 3. (a) Schematic illustration of the way to generate a simulated image. (b) One-dimensional explanation of generating procedure.

the observer just noticed the difference in sharpness and the width at that time was recorded. Ten observers participated in this experiment.

Figure 4 shows the experimental results. For each standard PSF (horizontal axis) the width of the test PSF at which seven or more observers noticed the difference is plotted. This result shows that a difference in FWHM larger than about 0.5 [pixels] makes it highly probable that observers will notice the difference. According to this result, the two CRTs mentioned above will have the same apparent sharpness to observers. On the other hand, they would distinguish the image produced by the film recorder from those on CRTs. This result gives us a motivation for sharpness matching and also yields criteria for judging whether the preprocessing for matching is needed for two given devices whose PSFs are known.

### 3. Formulation

Assuming a linear display system, we now formulate the display process and preprocessing technique. An original discrete image is represented by  $f_{mn}$  for  $m, n=1, 2, \dots, N$  where  $N$  is the number of columns or rows of the square image. For convenience, we redefine the original discrete image in continuous space by an array of discretely placed Dirac delta functions, i.e.,

$$f_s(x, y) = f(x, y) \text{comb}\left(\frac{x}{d}, \frac{y}{d}\right), \quad (1)$$

where  $d$  is the distance between neighboring pixels. The function  $f(x, y)$  represents a continuous function that has a value of  $f_{mn}$  at coordinate  $(md, nd)$  and is bounded by the area  $\{(x, y) | 0 \leq x, y \leq Nd\}$ . The two-dimensional comb function is defined as,

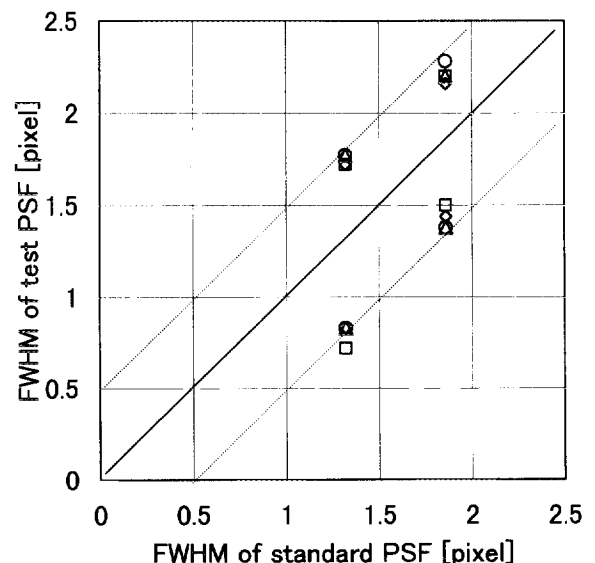


Fig. 4. Result of rating experiment. Each symbol represents one of sample images. FWHM of standard PSF is established at 1.32 and 1.86 [pixels].

$$\text{comb}\left(\frac{x}{d}, \frac{y}{d}\right) = \sum_{m=-\infty}^{\infty} \sum_{n=-\infty}^{\infty} \delta(x-md)\delta(y-nd).$$

Letting the PSF of the system be  $h(x, y)$ , we can represent the displayed image,  $f_d(x, y)$ , by the convolution of the PSF and the original discrete image:

$$\begin{aligned} f_d(x, y) &= f_s(x, y) * h(x, y) \\ &= \left[ f(x, y) \text{comb}\left(\frac{x}{d}, \frac{y}{d}\right) \right] * h(x, y), \end{aligned} \quad (2)$$

where  $*$  denotes a convolution operation. Eq. (2) can also be expressed in Fourier domain as

$$\begin{aligned} F_d(u, v) &= F_s(u, v)H(u, v) \\ &= [F(u, v) * \text{comb}(du, dv)]H(u, v). \end{aligned} \quad (3)$$

where  $F_d(u, v)$ ,  $F_s(u, v)$ ,  $F(u, v)$  and  $H(u, v)$  are the Fourier transform of  $f_d(x, y)$ ,  $f_s(x, y)$ ,  $f(x, y)$  and  $h(x, y)$ , respectively. The Fourier transform of  $\text{comb}(x/d, y/d)$  yields a multiplicative factor  $d^2$ . Here we omitted it for simplicity. In general,  $H(u, v)$  is a complex value. However, when  $h(x, y)$  has hermitian symmetric, which is reasonably assumed in many cases,  $H(u, v)$  becomes a real function.

If the system is completely continuous, the function  $H(u, v)$  has information about modulation and phase transfer for input sinusoidal function with spatial frequency of  $(u, v)$ . However, unlike optical imaging systems with lens, the digital image display system is not continuous in the sense that an original image is given discretely. Hence  $H(u, v)$  does not necessarily have such information about transfer. For instance, it does not have any physical meaning about transfer for sinusoidal functions in the frequency region above the Nyquist frequency ( $u, v = 1/2d$ ) because such a sinusoidal function can not be inherently defined as digital signal. The function  $H(u, v)$  still can be calculated at arbitrary frequency from the PSF. In this paper, we will call  $H(u, v)$  the transfer function for convenience and use it for preprocessing for sharpness matching without referring its physical meaning with respect to modulation and phase transfer.

Next, let us formulate the preprocessing technique. We assume two different display systems (system 1 and system 2) and represent the transfer function of each system by  $H_1(u, v)$  and  $H_2(u, v)$ . When the original discrete image  $f_s(x, y)$  is displayed with the two systems, the Fourier spectrum of displayed images,  $F_{1d}(u, v)$  and  $F_{2d}(u, v)$  are represented respectively as

$$F_{1d}(u, v) = F_s(u, v)H_1(u, v), \quad (4)$$

$$F_{2d}(u, v) = F_s(u, v)H_2(u, v). \quad (5)$$

If there is large difference between the two transfer functions, the displayed images could be observed with different sharpness. In order to make the output of system 2 close to that of system 1 (called the objective image here), we propose a filtering operation on the original digital image. The filter applied is based on the ratio of the two transfer functions. Mathematically, the ratio of the two transfer functions,  $R(u, v)$  is simply calculated by

$H_1(u, v)/H_2(u, v)$  for an arbitrary frequency as shown in Fig. 5(b). This idea is similar to the inverse filter used in, for example, deblurring.<sup>7</sup> However, because the filtering process is completely discrete, we are not able to apply  $R(u, v) = H_1(u, v)/H_2(u, v)$  to the region above the Nyquist frequency. Applying  $R(u, v) = H_1(u, v)/H_2(u, v)$  for the frequencies below the Nyquist frequency is equivalent to applying the following filter over entire frequency region, as shown in Fig. 5(c):

$$R(u, v) = \left\{ \frac{H_1(u, v)}{H_2(u, v)} \text{rect}(du, dv) \right\} * \text{comb}(du, dv), \quad (6)$$

where  $\text{rect}(du, dv)$  is a rectangular function defined as:

$$\text{rect}(du, dv) = \begin{cases} 1, & -1/2d < u, v < 1/2d \\ 0, & \text{otherwise.} \end{cases}$$

The Fourier spectrum of the discrete image after filtering is written as  $F_s(u, v)R(u, v)$ .

While the spatial frequency component below the Nyquist frequency are corrected by this filter properly, the other components are not corrected properly. In fact, the Fourier spectrum of the filtered and displayed image,  $F_{2c}(u, v)$  can be expressed as follows: for the frequency

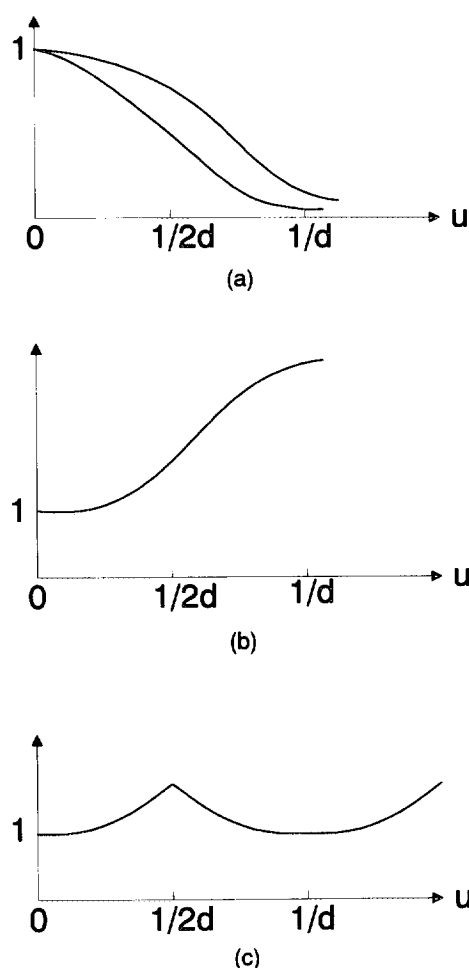


Fig. 5. Schematic illustration of (a) two transfer functions, (b) the ratio of those functions, and (c) practically applied filter.

region below the Nyquist frequency, i.e., for  $-1/2d \leq u, v \leq 1/2d$

$$F_{2c}(u, v) = [F_s(u, v)R(u, v)]H_2(u, v), \quad (7a)$$

and for the frequency region above the Nyquist frequency, i.e., for an arbitrary integer  $(m, n)$  except for  $(0, 0)$ , and  $-1/2d \leq u, v \leq 1/2d$ ,

$$F_{2c}\left(u + \frac{m}{2d}, v + \frac{n}{2d}\right) = F_s(u, v) \frac{H_1(u, v)}{H_2(u, v)} H_2\left(u + \frac{m}{2d}, v + \frac{n}{2d}\right). \quad (7b)$$

Namely, the spectrum of the filtered and displayed image is different from that of the objective image in the region

above the Nyquist frequency. Practically, however, this difference is almost negligible because the higher frequencies inherently contain much less power than the lower frequencies and therefore do not affect image quality so much. An overall, schematic illustration is shown, in one dimension for simplicity, in Fig. 6 to explain the above model.

The filter  $R(u, v)$  might be a high pass filter (HPF) or might be a low pass filter (LPF). It depends on which system of the two is the objective one in the matching operation. Usually users will want to obtain a sharper image with a system that is worse in a sense of sharpness. The idea introduced here, however is rather general and

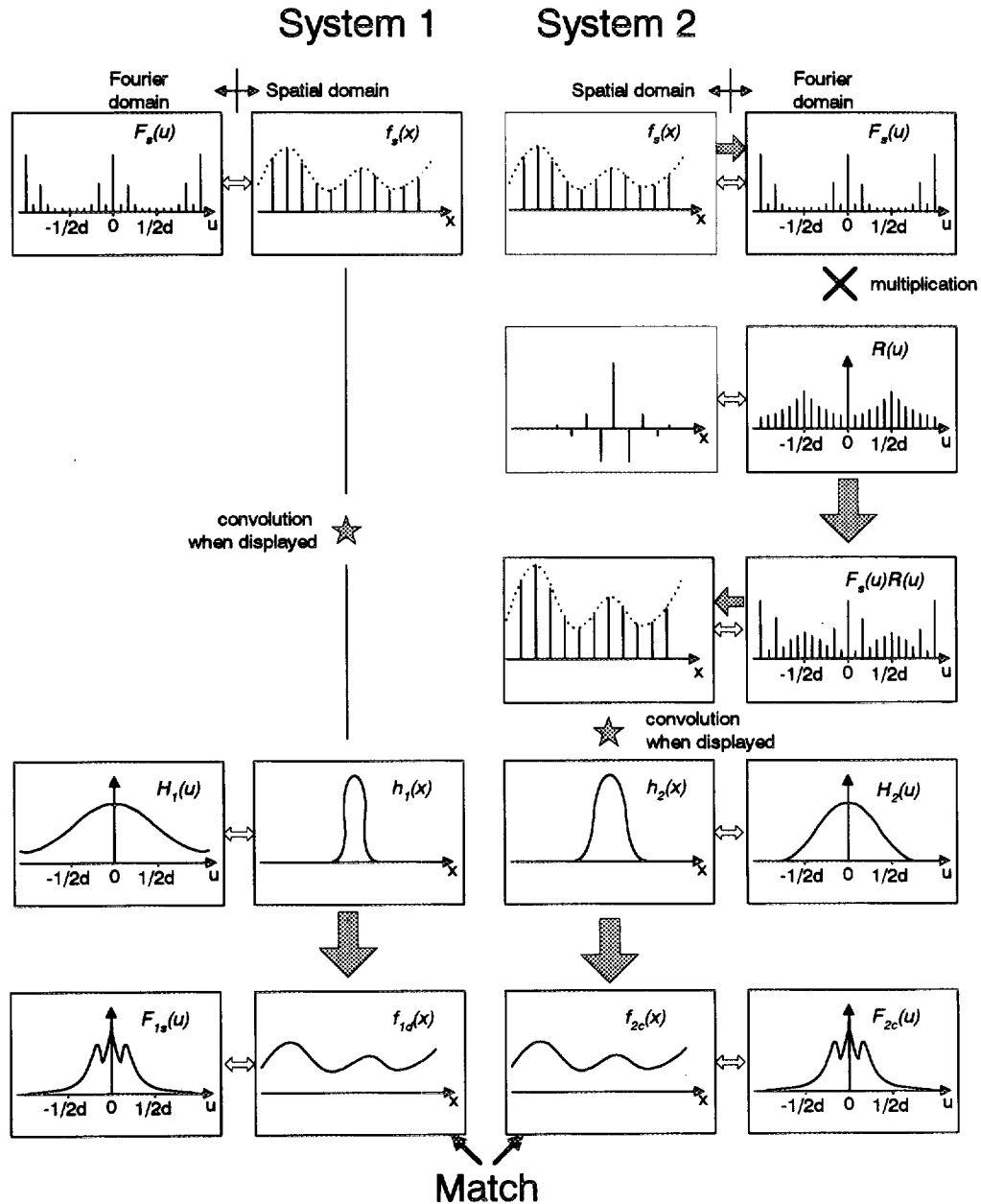


Fig. 6. Schematic diagram of the correction procedure. Correction and display process are denoted by gray arrows. Fourier transform pairs at each step are denoted by blank arrows.

can be applied to either case.

In fact, we omitted one important point in the above model. It is that after filtering, the pixel value of the digital images might be out of the quantization levels allowed in the system. For instance, if the D/A converter of display device has 8 bit-level, the pixel value ranges from 0 to 255. If the values of filtered image exceed this range, those values must be clipped. The resulting digital image,  $f_p(x, y)$  is then written as

$$f_p(x, y) = O_c\{f_f(x, y)\} = \begin{cases} 255, & 255 < f_f(x, y) \\ f_f(x, y), & 0 \leq f_f(x, y) \leq 255, \\ 0, & f_f(x, y) < 0 \end{cases} \quad (8)$$

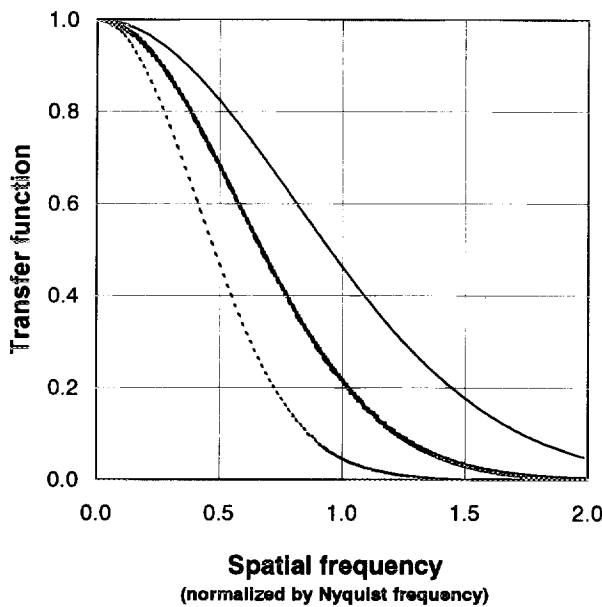


Fig. 7. PSFs of the systems assumed in the simulation. —, A; ---, B; ···, C.

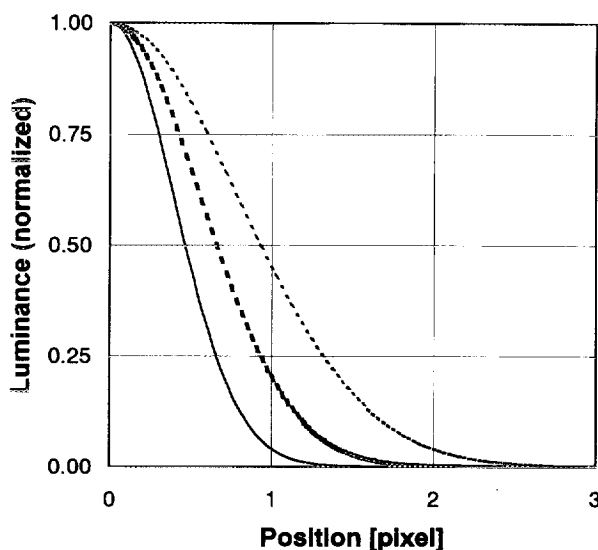


Fig. 8. Transfer functions obtained from Fourier transform of PSFs in Fig. 7.

where  $O_c\{\cdot\}$  denotes an operator representing clipping operation. The function  $f_f(x, y)$  is the digital image obtained after filtering and inverse Fourier transformation, i.e.,

$$f_f(x, y) = \mathcal{F}^{-1}\{F_s(u, v)R(u, v)\}, \quad (9)$$

where  $\mathcal{F}^{-1}$  denotes inverse Fourier transform.

If the excess of the range is too large, the filtering results in degrading rather than correcting the image. Such degradation may occur when the filter has HPF characteristic and its gain is too large. Thus it is necessary to control the gain of the filter properly. As a simple technique, we adopted a clipping operation in Fourier domain. Namely, the clipped filter  $R_c(u, v)$  is written as

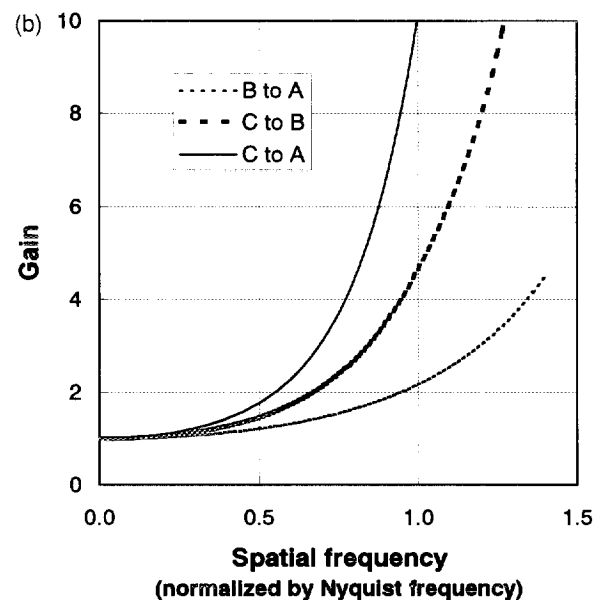
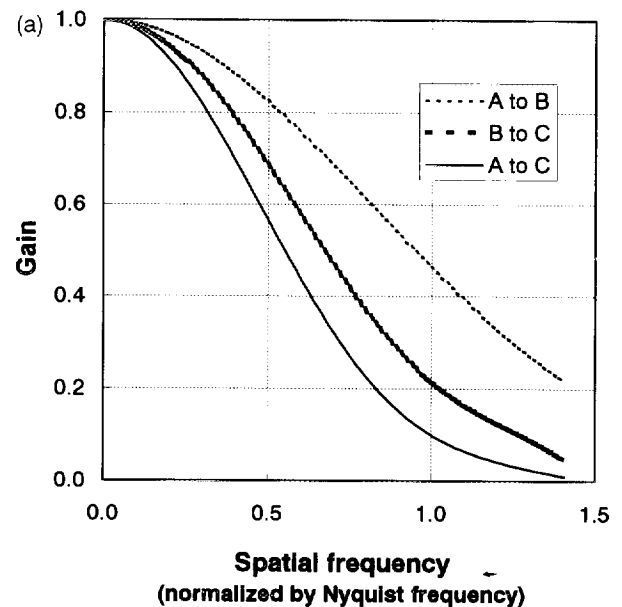


Fig. 9. Ratio of transfer functions, (a) LPFs, (b) HPFs.

$$R_c(u, \nu) = \begin{cases} T, & T < R(u, \nu) \\ R(u, \nu), & \text{otherwise} \end{cases} \quad (10)$$

where  $T$  means a predetermined clipping level. Ultimately, the Fourier spectrum of the displayed image after correction can be expressed as:

$$F_{2c}(u, \nu) = \mathcal{F}\{O_c\{\mathcal{F}^{-1}\{F_s(u, \nu)R_c(u, \nu)\}\}H_2(u, \nu)\}. \quad (11)$$

Finally we will discuss how to determine the clipping level,  $T$ . Because both clipping operations in Fourier

domain and spatial domain are image dependent, non-linear processing, it is not easy to find an optimum clipping level. A following procedure using computer simulation is one possible way: first establish an objective function for evaluating the goodness of corrected image, second generate simulated images, third evaluate the function and correct  $T$  so as to minimize it. For this purpose, we consider that the following function is useful<sup>8)</sup>:

$$V = \frac{\sum_u \sum_\nu |F_{1d}(u, \nu) - F_{2c}(u, \nu)| H_{eye}(u, \nu)}{\sum_u \sum_\nu |F_{1d}(u, \nu)| H_{eye}(u, \nu)}, \quad (12)$$

where  $H_{eye}(u, \nu)$  represents the contrast sensitivity function of human visual system. The evaluation function is given by the amplitude of the difference between Fourier spectra of two images weighted by  $H_{eye}(u, \nu)$  with a band pass characteristic. The denominator for normalization in the equation is not important for finding the optimum threshold level. The introduction of  $H_{eye}(u, \nu)$  is significant in order that the resulting numerical evaluation has good correlation with subjective evaluation by human observer. In the computer simulation, we used the above measure to evaluate the degree of correction.

#### 4. Computer Simulation

Assuming three systems with different PSFs, we generated simulated images and evaluated the degree of sharpness matching numerically. The PSFs were given by two-dimensional, symmetric Gaussian function and convolved with discrete images to generate simulated images in the same manner as the preliminary experiment. The three systems, A, B and C, have the PSFs of 0.93, 1.32 and 1.86 FWHM, respectively. The cross sections of these PSFs and the corresponding transfer functions are shown in Figs. 7 and 8, respectively. For these systems, we examined every combination of matching, namely A to B, B to A, B to C, C to B, C to A and A to C, where "X to Y"

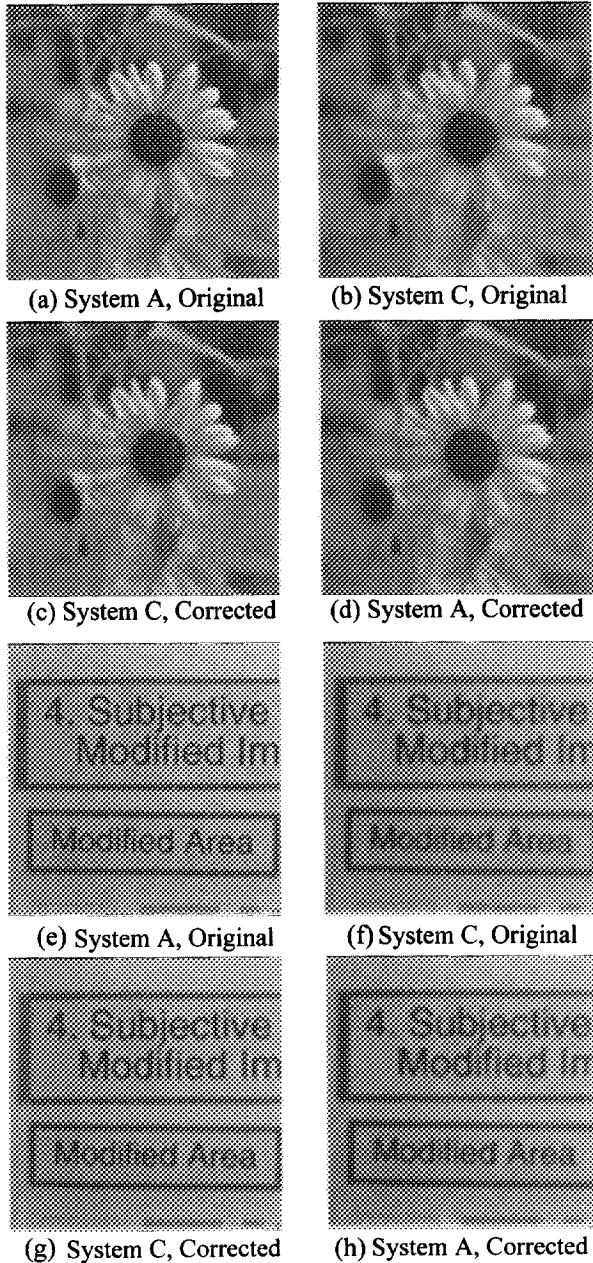


Fig. 10. Example of simulated images. (a), (e): Images displayed in system A without correction. (b), (f): Images displayed in system C without correction. (c), (g): Images displayed in system C after being corrected so as to match to system A. (d), (h): Images displayed in system A after being corrected so as to match to system C.

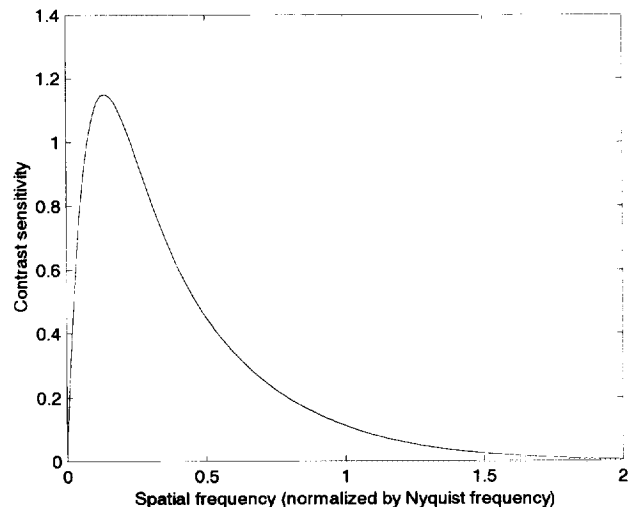


Fig. 11. Contrast sensitivity of human visual system used in numerical evaluation.

means that the image to be displayed on system  $X$  is corrected so that it matches to the image displayed on system  $Y$ . Three of these combinations correspond to low pass filtering and the others correspond to high pass filtering. Figures 9(a) and (b) show the ratios of transfer functions which are used as filter functions.

The four images shown in Sect. 2 were used as original images for this simulation. Figure 10 shows two sets of simulated images, where (a), (e) and (b), (f) are the images displayed without correction on system A and C, respectively. Figures 10(c), (g) are the images displayed on system C after being corrected so as to match to system A. The images (d), (h) are the opposite case of (c), (g). In the processing to obtain (c), (g), a proper clipping operation in Fourier domain was carried out. We can see that each

corrected image became closer to the respective upper image than non-corrected image.

We evaluated the degree of sharpness matching by Eq. (12). The visual contrast sensitivity function,  $H_{eye}(u, v)$  was approximated by the following analytical function,<sup>8,9)</sup>

$$H_{eye}(u, v) = aU \exp(-bU) \sqrt{1 + c \exp(bU)}, \quad (13)$$

where

$$U = \frac{\pi R D \sqrt{u^2 + v^2}}{180 \times S}$$

$$a = 440(1 + 0.7/L)^{-0.2}$$

$$b = 0.3(1 + 100/L)^{0.15}$$

$$c = 0.06.$$

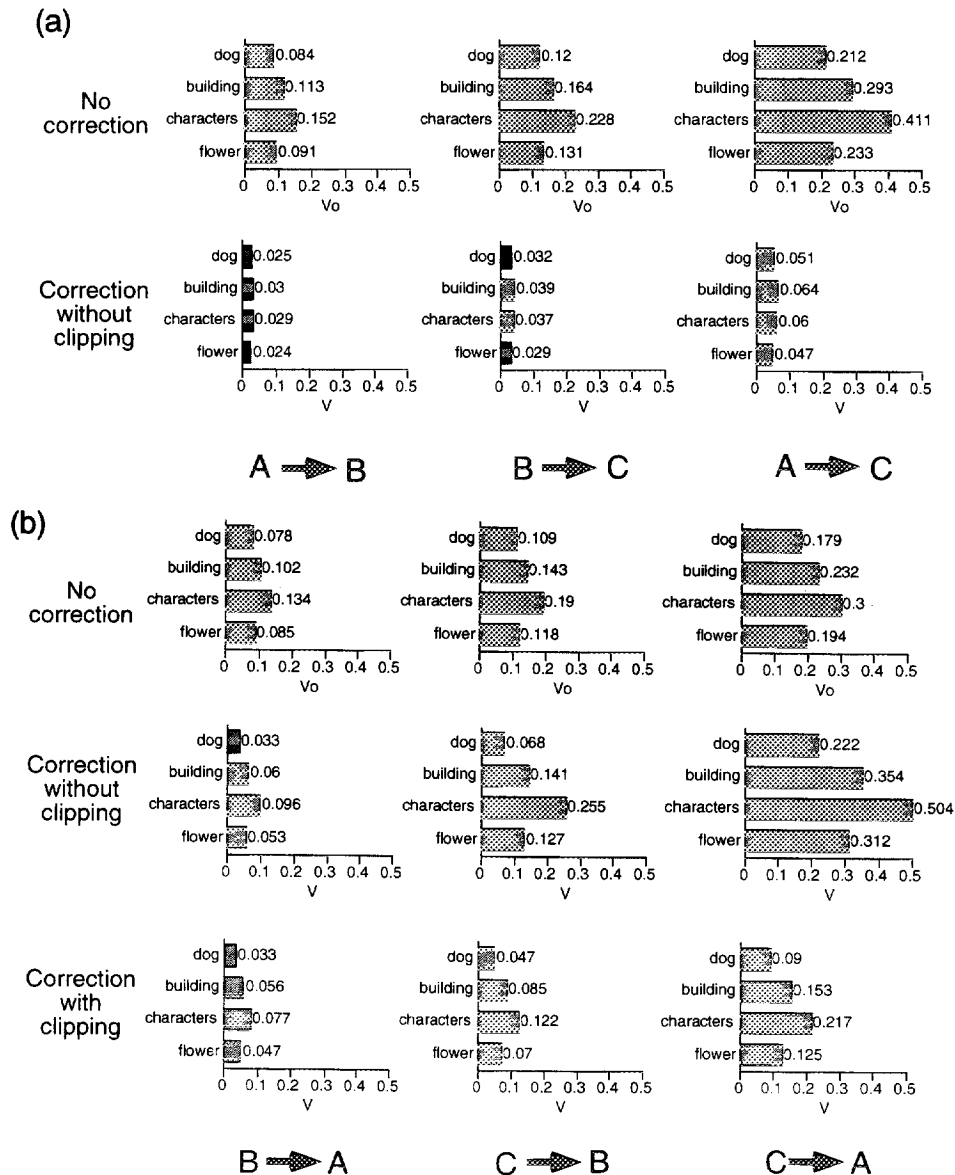


Fig. 12. Numerical evaluation results. (a) LPF cases. (b) HPF cases. First row corresponds to Eq. (14). Second row corresponds to Eq. (12) without clipping operation. Third row corresponds to Eq. (12) with proper clipping operation.



In the above equation, the parameters  $R$ ,  $D$ ,  $S$  and  $L$  represent, resolution of display [dot/mm], viewing distance [mm], size of image width [pixel], and maximum luminance of display [cd/m<sup>2</sup>], respectively. The values of these parameters were set as  $R=2.35$  [dot/mm],  $D=750$  [mm],  $S=1024$  [pixel], and  $L=63.0$  [cd/m<sup>2</sup>]. The values of  $R$ ,  $S$  and  $L$  were determined by referring to the specification of CRT A. Figure 11 shows a visual contrast sensitivity function used, where horizontal axis is normalized by the Nyquist frequency.

Figures 12(a), (b) show evaluation values calculated, where each three columns of (a) and (b) correspond to LPF and HPF cases, respectively. We first calculated the difference between the images which are both displayed without correction by the following equation:

$$V_o = -\frac{\sum_u \sum_v |F_{1d}(u, v) - F_{2d}(u, v)| H_{eye}(u, v)}{\sum_u \sum_v |F_{1d}(u, v)| H_{eye}(u, v)}. \quad (14)$$

This equation is the same as Eq. (12) except that  $F_{2c}(u, v)$  is replaced by the Fourier spectrum of original image,  $F_{2d}(u, v)$ . The first row in Figs. 12(a) and (b) represents the results calculated by Eq. (14). The second row represents the results with correction using the basic filter Eq. (6). In the LPF cases (Fig. 12(a)), the correction works successfully and the corrected images are very close to the objective images. On the other hand, in the HPF cases (Fig. 12(b)) the corrected images are not necessarily better than non-corrected images. Especially, in the case of "C to A," the corrected images were all worse than the non-corrected images. This is due to the clipping operation in spatial domain resulting from the excessive enhancement in HPF. In fact, for the case of "C to A" we tried to remove the limitation of quantization levels and simulate displayed images. This simulation is not physically feasible but useful to confirm the effect of the limitation. As a result, the generated images were close to the objective images and the values of evaluation functions for 'flower,' 'characters,' 'building' and 'dog' were 0.06, 0.075, 0.102, and 0.076 respectively.

We therefore need to introduce the clipping operation for HPFs. Since it was difficult to know in advance which clipping level is optimum, we decided to try many clipping levels and evaluate the results. The range from 1 to 4 of clipping level was examined in the interval of 0.25. Figure 13 shows the results. According to these results, for every case, clipping levels around 1.5 give good results. A small variation is observed in the character image and dog image, i.e., in the character image the optimum clipping level is a little lower than others. In the dog image it is a little higher than others. This variation results from the difference in magnitude of high spatial frequency components. The character image has larger power in high spatial frequency than others and the dog image has less power than others. Although there is a little variation, the choice of clipping level seems rather robust. Figure 14 shows two sets of images with various clipping levels in the case of "C to A." While the image without clipping

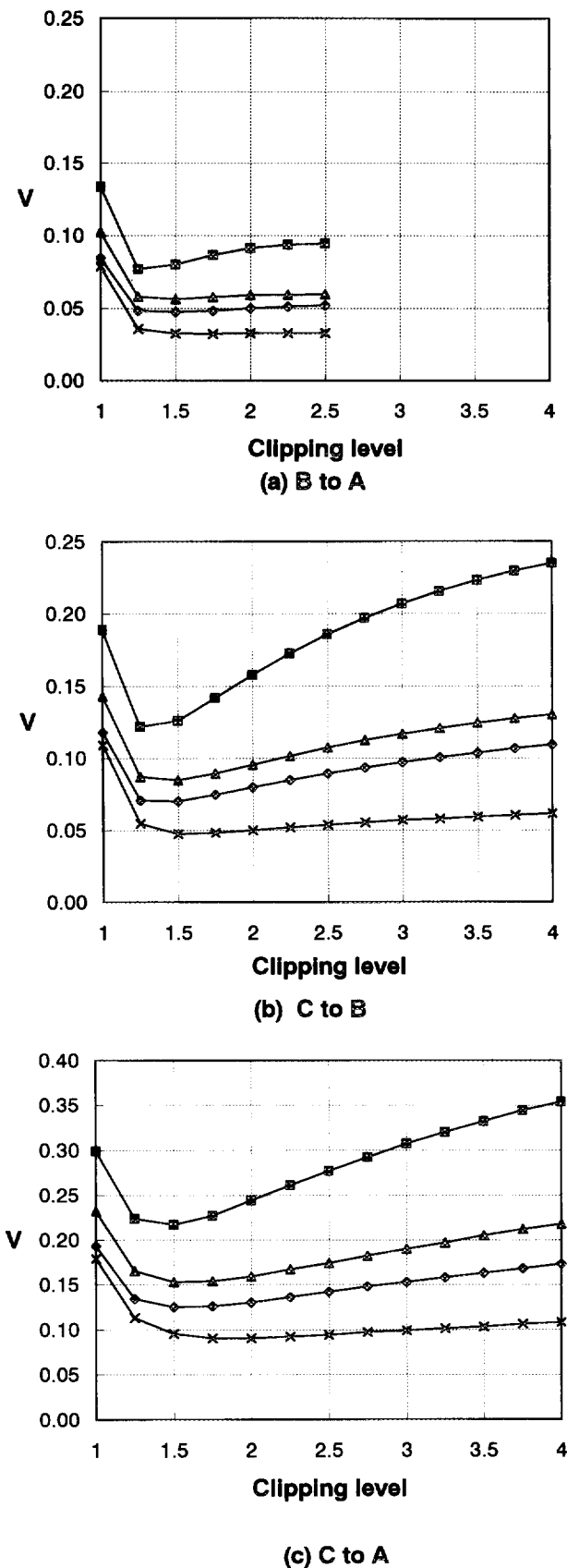


Fig. 13. Relationship between clipping level and degree of matching,  $V$ . (a) B to A, (b) C to B, (c) C to A. ♦, flower; ■, characters; ▲, building; ×, dog.

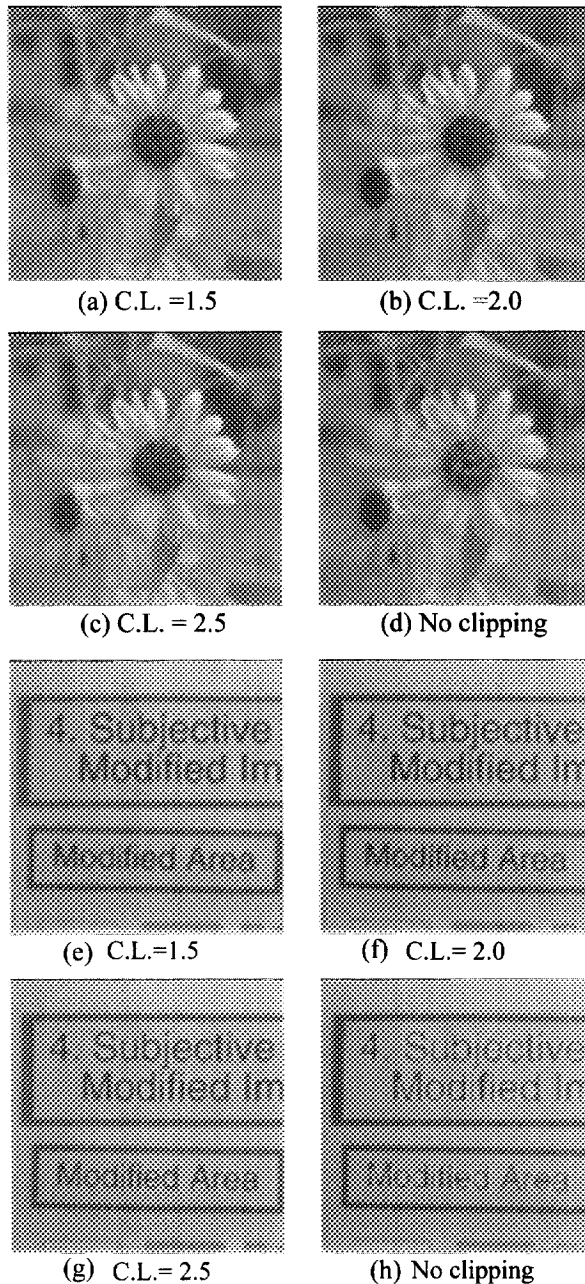


Fig. 14. Images obtained with different clipping levels. Clipping levels of (a) and (e), (b) and (f), (c) and (g) are 1.5, 2.0 and 2.5, respectively. (d) and (h) correspond to no clipping operation.

operation is highly degraded, the images with clipping levels near 1.5 are similar one another. Thus, the above clipping level seems to be applicable to a variety of images. Even if the above values do not provide good result, the user can find the optimum value using Eq. (12).

The third row in Fig. 12(b) represents the best results obtained with proper clipping operation. In the case of "B to A," we did not find a significant improvement because the basic filter Eq. (6) does not have large gain. On the other hand, in the cases of "C to B" and "C to A," we find a significant improvement.

Table 2. Statistics in the width of PSF of CRT B.

	Input level	Horizontal	Vertical
64	ave.	1.76	1.36
	s.d.	0.15	0.20
128	ave.	1.64	1.53
	s.d.	0.11	0.25
255	ave.	1.74	1.69
	s.d.	0.33	0.45
Total	ave.	1.71	1.53
	s.d.	0.22	0.34

## 5. Discussion

In the preliminary experiment, the simulated images were displayed and compared on the same CRT. This experiment implicitly assumes that the luminance range of two different systems tested is the same. In every numerical evaluation using Eqs. (12), (13), we also used the same value for parameter  $L$  in Eq. (13). This evaluation is based on the assumption that the maximum luminance of any two different systems is the same. However, in case of X-ray film viewer and CRT, for example, there exists a big difference in the maximum luminance.<sup>10)</sup> The results obtained might not be directly applied to such a case. Though we believe that the proposed concept is still useful for a variety of applications, we suggest that users consider whether the obtained results are applicable to their specific two systems.

In the computer simulation, we assumed that the PSF was linear, symmetric and globally space invariant or uniform (The PSF is, of course, locally space variant because it is defined only at the locations where dots are placed). This assumption should be reconsidered as well. Obviously, when the PSF is globally space invariant, the proposed method using the Fourier transform is still available even if the PSF is asymmetric. However, when the PSF is globally space variant and/or non-linear, a different mathematical model and correction technique are required. Thus, we investigated the degree of uniformity and linearity of a typical, real display system. The CRT B described in Sect. 2 was used for this investigation. One pixel was displayed at nine positions on the screen with input levels of 64, 128 and 255 (maximum). From the images of the PSFs, we measured the horizontal and vertical FWHM.

Table 2 shows the first and second order statistics calculated, i.e., the average and standard deviation of the width for each input level, and average and standard deviation of the total data (nine positions  $\times$  three input levels). The standard deviation at each input level represents the non-uniformity and difference between averages at each input level represents the non-linearity. We can see some degree of variation in the width of PSF with respect to both position and input level. Here, let us recall the result of the preliminary experiment. It shows that the difference within about 0.5 [pixel] of width is not noticeable and is acceptable for observers. The values of the standard deviation in Table 2 are comparable with or smaller than this

level. The sharpness matching is required for the systems with larger difference than this level, and for such systems, a slight lack of uniformity and linearity as shown here is probably negligible.

We will further show the mathematical expression and correction technique for the case that the non-uniformity and non-linearity are not negligible. When the PSF is non-uniform, filtering has to be carried out in the spatial domain rather than the Fourier domain. We use vector-matrix notation to represent the imaging and processing model for such a case. A two dimensional digital image is represented by a vector  $\mathbf{f}$  whose elements are arranged in raster scan order. For a two dimensional image with  $N \times N$  pixels, therefore the dimension of  $\mathbf{f}$  is  $N^2 \times 1$ . On the other hand, we assume that continuous display area is finely sampled and represented by  $M \times M$  points ( $M > N$ ). Then, a displayed image is represented by a vector  $\mathbf{g}$  with a dimension of  $M^2 \times 1$ . The display system can be approximated by a matrix  $\mathbf{H}$  whose  $(i, j)$  element represents the contribution of  $j$ th pixel of the image to  $i$ th position in display area. Thus, the dimension of the system matrix  $\mathbf{H}$  is  $M^2 \times N^2$ . When the system is linear, the displayed image  $\mathbf{g}$  can be approximated by multiplication of  $\mathbf{H}$  and  $\mathbf{f}$  as:

$$\mathbf{g} = \mathbf{H}\mathbf{f}. \quad (15)$$

If the system is non-linear, the elements of system matrix  $\mathbf{H}$  are not constant any more but depend on the input image,  $\mathbf{f}$ .

To match two images, we establish an evaluation function again. Denoting the filter to be designed by a matrix  $\mathbf{R}$  with dimension of  $N^2 \times N^2$ , we can write the filtering operation as  $\mathbf{R}\mathbf{f}$ . If the pixel values of corrected image are outside of the quantization levels, those values are still clipped. Denoting the system matrixes be  $\mathbf{H}_1$  and  $\mathbf{H}_2$ , and introducing the human contrast sensitivity function as  $\mathbf{H}_{\text{eye}}$ , we can give one possible evaluation function by:

$$V = \|\mathbf{H}_{\text{eye}}(\mathbf{H}_1\mathbf{f} - \mathbf{H}_2\mathbf{O}_c\{\mathbf{R}\mathbf{f}\})\|, \quad (16)$$

where  $\|\cdot\|$  denotes a vector norm. Each column of  $\mathbf{H}_{\text{eye}}$  is a convolution operator with a band pass characteristic corresponding to human visual perception. If the systems are non-linear, the elements of  $\mathbf{H}_1$  and  $\mathbf{H}_2$  are still dependent on input images,  $\mathbf{f}$  and  $\mathbf{O}_c\{\mathbf{R}\mathbf{f}\}$ , respectively.

The above expression is a generalization of the originally proposed method. Though the evaluation function to be minimized was shown, practical minimization requires rather difficult computation. In fact, each matrix in the equation is quite large, and because of nonlinear operations including clipping, sophisticated optimization algorithms may be not applied. We successfully applied the one-dimensional version of this technique to correction of non-uniformity in a fluorescent type color printer.<sup>11)</sup> This problem was much easier than the two dimensional ver-

sion. Practical implementation should be developed for systems with highly non-linear and/or non-uniform PSFs in future.

Finally, the proposed method is based on the measurement of the PSF of the system. However, it is not easy task for general users. Thus, for this purpose, it is desired that the developer of the display device presents the data about the PSF as well as the spatial resolution.

## 6. Conclusions

We have proposed a method for matching the appearance of sharpness between different display devices. The method is basically a spatial filtering using information about the transfer function of each device. We first investigated the width of PSFs of a few practical devices and found that there is a large difference (0.9 at maximum) which is greater than the difference level that the human visual system just notices.

We formulated the imaging model and matching operation and pointed out a problem due to the limited range of pixel values. We proposed a clipping operation in the Fourier domain, which functions well to achieve reasonable image quality when a filter has a high pass characteristic with a large gain. Through computer simulation and numerical evaluation with four images, we demonstrated the effectiveness of the filtering operation for sharpness matching. We found that in HPF, a clipping level of 1.5 provides good matching for all prepared images.

Because the concept of the proposed method is quite general, we believe it is widely applicable to a variety of fields including clinical field. On the other hand, we introduced some assumptions in computer simulation. Thus, as a future work, the influence of these assumptions should be examined using practical devices.

## References

- 1) H. Haneishi, K. Miyata, H. Yaguchi and Y. Miyake: *J. Imaging Sci. Technol.* **37** (1993) 30.
- 2) H. Haneishi, R. Ohtake, Y. Miyake and P.C. Hung: *Proc. Non-Impact Printing* (1994) p. 561.
- 3) T. Mertemeier and T.E. Kocher: *Proc. SPIE* **2707** (1996) 33.
- 4) T.L. Ji: Ph.D Thesis, The University of Arizona (1993).
- 5) C. Infante: *Proc. SID, Seminar* (1994) M-7.
- 6) H. Haneishi, T. Shiobara and Y. Miyake: *Opt. Commun.* **114** (1995) 57.
- 7) R.C. Gonzalez and R.E. Woods: *Digital Image Processing* (Addison-Wesley, Massachusetts, 1992) p. 270.
- 8) N. Tsumura, K. Sanpei, H. Haneishi and Y. Miyake: *Proc. of IS&T's 49th Annual Conference* (1996) p. 312.
- 9) Peter G.J. Barten: *IEEE Trans. Electron Devices* **36** (1989) 1865.
- 10) H. Blume, H. Roehrig, M. Browne and T.L. Ji: *Proc. SPIE* **1232** (1990) 97.
- 11) H. Haneishi, T. Tsukagoshi and Y. Miyake: *IEICE J78-DII* (1995) 1721.